ELSEVIER
Physics Letters B 527 (2002) 161–172
www.elsevier.com/locate/npe

Measurement of $e^+e^- \to \pi^+\pi^-$ cross-section with CMD-2 around ρ-meson

R.R. Akhmetshin [a], E.V. Anashkin [a], A.B. Arbuzov [b], V.M. Aulchenko [a,c], V.Sh. Banzarov [a], L.M. Barkov [a], S.E. Baru [a], N.S. Bashtovoy [a], A.E. Bondar [a,c], D.V. Bondarev [a], A.V. Bragin [a], D.V. Chernyak [a], S. Dhawan [e], S.I. Eidelman [a,c], G.V. Fedotovich [a,c], N.I. Gabyshev [a], D.A. Gorbachev [a,c], A.A. Grebenuk [a], D.N. Grigoriev [a,c], V.W. Hughes [e], F.V. Ignatov [a,c], S.V. Karpov [a], V.F. Kazanin [a], B.I. Khazin [a,c], I.A. Koop [a,c], P.P. Krokovny [a], E.A. Kuraev [b], L.M. Kurdadze [a], A.S. Kuzmin [a,c], I.B. Logashenko [a,d], P.A. Lukin [a], A.P. Lysenko [a], K.Yu. Mikhailov [a], J.P. Miller [d], A.I. Milstein [a,c], I.N. Nesterenko [a], V.S. Okhapkin [a], A.A. Polunin [a], A.S. Popov [a], T.A. Purlatz [a], B.L. Roberts [d], N.I. Root [a], A.A. Ruban [a], N.M. Ryskulov [a], A.G. Shamov [a], Yu.M. Shatunov [a], B.A. Shwartz [a,c], A.L. Sibidanov [a], V.A. Sidorov [a], A.N. Skrinsky [a], V.P. Smakhtin [a], I.G. Snopkov [a], E.P. Solodov [a,c], P.Yu. Stepanov [a], A.I. Sukhanov [a], J.A. Thompson [f], V.M. Titov [a], Yu.Y. Yudin [a], S.G. Zverev [a]

[a] *Budker Institute of Nuclear Physics, Novosibirsk, 630090, Russia*
[b] *Joint Institute of Nuclear Research, Dubna, 141980, Russia*
[c] *Novosibirsk State University, Novosibirsk, 630090, Russia*
[d] *Boston University, Boston, MA 02215, USA*
[e] *Yale University, New Haven, CT 06511, USA*
[f] *University of Pittsburgh, Pittsburgh, PA 15260, USA*

Received 14 December 2001; received in revised form 21 December 2001; accepted 8 January 2002

Editor: L. Montanet

Abstract

The cross-section of the process $e^+e^- \to \pi^+\pi^-$ has been measured using about 11 4000 events collected by the CMD-2 detector at the VEPP-2M e^+e^- collider in the center-of-mass energy range from 0.61 to 0.96 GeV. Results of the pion form factor determination with a 0.6% systematic uncertainty are presented. The following values of the ρ- and ω-meson parameters were found: $M_\rho = (776.09 \pm 0.81)$ MeV, $\Gamma_\rho = (144.46 \pm 1.55)$ MeV, $\Gamma(\rho \to e^+e^-) = (6.86 \pm 0.12)$ keV, $\mathrm{Br}(\omega \to \pi^+\pi^-) = (1.33 \pm 0.25)\%$. Implications for the hadronic contribution to the muon anomalous magnetic moment are discussed.

E-mail address: simon.eidelman@cern.ch (S.I. Eidelman).

0370-2693/02
PII: S0370-2693(02)01168-1

1. Introduction

The cross-section of the process $e^+e^- \to \pi^+\pi^-$ is usually expressed in terms of the pion electromagnetic form factor $F_\pi(s)$:

$$\sigma_{e^+e^-\to\pi^+\pi^-} = \frac{\pi\alpha^2}{3s}\beta_\pi^3 \left|F_\pi(s)\right|^2, \tag{1}$$

where s is the center-of-mass (c.m.) energy squared, m_π is the pion mass and $\beta_\pi = \sqrt{1-4m_\pi^2/s}$ is the pion velocity in the c.m. frame.

The pion form factor measurement is crucial for a number of physics problems. Detailed experimental data in the time-like region allow a determination of the parameters of the $\rho(770)$ meson and its radial excitations. Extrapolation of the energy dependence of the pion form factor to the point $s = 0$ provides a value of the pion electromagnetic radius.

In the energy range below $\phi(1020)$ the process $e^+e^- \to \pi^+\pi^-$ gives the dominant contribution to the quantity $R(s)$ defined as

$$R = \frac{\sigma(e^+e^- \to \text{hadrons})}{\sigma(e^+e^- \to \mu^+\mu^-)}.$$

$R(s)$ is an important measurable quantity widely used for various QCD tests as well as calculations of the dispersion integrals. For such applications, at high energies $R(s)$ is usually calculated within the perturbative QCD frame, while for the low energy range the direct measurement of the $e^+e^- \to$ hadrons cross-section is necessary.

Particularly, knowledge of $R(s)$ with high accuracy is required for the evaluation of the hadronic contribution a_μ^{had} to the anomalous magnetic moment of the muon $(g-2)/2$ (see [1] and references therein). The ultimate goal of the experiment E821 [2] running in Brookhaven National Laboratory is to measure the muon anomalous magnetic moment with a relative precision of 0.35 ppm. Within the Standard Model (SM) the uncertainty of the theoretical value of the leading order a_μ is dominated by the uncertainty of the hadronic contribution a_μ^{had} calculated via the dispersion integral

$$a_\mu^{\text{had}} = \left(\frac{\alpha m_\mu}{3\pi}\right)^2 \int\limits_{4m_\pi^2}^{\infty} \frac{R(s)K(s)}{s^2}\,ds = \frac{m_\mu^2}{12\pi^3}\int\limits_{4m_\pi^2}^{\infty} \frac{\sigma(s)K(s)}{s}\,ds, \tag{2}$$

where $K(s)$ is the QED kernel and $\sigma(s)$ is the cross-section of $e^+e^- \to$ hadrons. The precision of the a_μ^{had} calculation depends on the approach used and varies from 1.34 ppm based on e^+e^- data only [3] to 0.53 ppm if in addition τ-lepton decay data as well as perturbative QCD and QCD sum rules are extensively used [4]. The major contribution to its uncertainty comes from the systematic error of the $R(s)$ measurement at low energies ($s < 2$ GeV^2), which, in turn, is dominated by the systematic error of the measured cross section $e^+e^- \to \pi^+\pi^-$.

Assuming conservation of the vector current (CVC) and isospin symmetry, the spectral function of the $\tau^- \to \pi^-\pi^0\nu_\tau$ decay can be related to the isovector part of the pion form factor [5]. The detailed measurement of the spectral functions was provided by ALEPH [6], OPAL [7] and CLEO-II [8]. The comparison of the pion form factor measured at e^+e^- colliders with the spectral function of the $\tau^- \to \pi^-\pi^0\nu_\tau$ decay provides a test of CVC. If CVC holds with high accuracy, τ-lepton decay data can be also used to improve the accuracy of the calculations mentioned above [9,10].

E821 has recently published the result of its measurement of a_μ with an accuracy of 1.3 ppm [11]. The measured value of a_μ is 2.6 standard deviations higher than the SM prediction of [4].[1] This observation makes new high precision measurements of the $e^+e^- \to$ hadrons cross-section and particularly of the pion form factor extremely important.

Since early 70s the VEPP-2M e^+e^- collider has been running in the Budker Institute of Nuclear Physics in the c.m. energy range 360–1400 MeV. The most precise pion form factor data were obtained in late 70s–early 80s by CMD and OLYA detectors [13]. Their accuracy was limited by systematic errors of the

[1] Recent progress in estimating the light-by-light scattering contribution to a_μ^{had} [12] implies that the difference between experiment and theory reduces to about 1.5 standard deviations.

experiments, varying from 2 to 15% over the VEPP-2M energy range.

The CMD-2 detector installed in 1991 is a general purpose detector consisting of the drift chamber, the proportional Z-chamber, the barrel CsI calorimeter, the endcap BGO calorimeter installed in 1996, and the muon range system. The drift chamber, Z-chamber and the endcap calorimeters are placed inside a thin superconducting solenoid with a field of 1 T. More detail on the detector can be found elsewhere [14].

Though the collider luminosity has not considerably increased since the previous work in the 1980s, the present detector design is significantly improved, resulting in a smaller systematic error of the pion form factor in this measurement. Particularly, the following advantages of CMD-2 should be mentioned compared to previous detectors: simultaneous measurement of the particle momentum and energy deposition which simplified particle identification and helped to reduce background; high precision determination of the fiducial volume with the help of the Z-chamber; a thinner beam pipe which reduced the nuclear interactions of pions.

During 1994–1995 a detailed scan of the c.m. energy range 610–960 MeV was performed. Since the pion form factor changes relatively fast in this energy range dominated by the ρ-meson, the systematic error due to an uncertainty in the energy measurement can be significant. To reduce this contribution to a negligible level, the beam energy was measured with the help of the resonance depolarization technique with an accuracy of 140 keV for almost all energy points [15]. This Letter presents the final analysis of the data taken in 1994–1995 with the integrated luminosity of about 310 nb^{-1} and a systematic uncertainty of the cross section of 0.6%. Preliminary results with a systematic uncertainty of 1.4% were published in [16], based on the same data sample.

2. Data analysis

The data were collected at 43 points with c.m. energy ranging from 610 to 960 MeV in 10 MeV energy steps, except for the narrow energy range near the ω-meson, where the energy steps were 2–6 MeV.

From more than 4×10^7 triggers recorded, about 3×10^5 events were selected as *collinear*, with a signature of two particles of opposite charge and nearly back-to-back momenta originating from the interaction point. The following selection criteria were used:

(1) Two tracks of opposite charge originating from the interaction region are reconstructed in the drift chamber.
(2) The distance from the vertex to the beam axis, ρ, is less than 0.3 cm and the z-coordinate of the vertex (along the beam axis) is within $-15 < z < 15$ cm.
(3) The average momentum of the two particles $(p_1 + p_2)/2$ is between 200 and 600 MeV/c.
(4) The difference between the azimuthal angles (in the plane perpendicular to the beam axis) of two particles $|\Delta\varphi| = |\pi - |\varphi_1 - \varphi_2|| < 0.15$.
(5) The difference between the polar angles (the angle between the momentum and the beam axis) of two particles $|\Delta\Theta| = |\Theta_1 - (\pi - \Theta_2)| < 0.25$.
(6) The average polar angle of two particles $\Theta_{\mathrm{avr}} = [\Theta_1 + (\pi - \Theta_2)]/2$ is within $1.1 < \Theta_{\mathrm{avr}} < (\pi - 1.1)$. This criterion determines the fiducial volume.

The selected sample of collinear events contains $e^+e^- \to e^+e^-$, $e^+e^- \to \pi^+\pi^-$, $e^+e^- \to \mu^+\mu^-$ events (below referred to as beam originating) as well as the background of cosmic particles which pass near the interaction region and are misidentified as collinear events. The number of cosmic background events N_{cosmic} was determined by the analysis of the spatial distribution of the vertex. Both distributions of the longitudinal coordinate (z) and the distance from the beam axis (ρ) are peaked around zero for the beam originating events, but are very broad, almost flat for the cosmic background events. Typical ρ- and z-distributions are shown in Fig. 1.

The momenta of e, μ, π from the beam originating events are rather close (the difference is comparable to the momentum resolution of the drift chamber), so the overlap of the momentum distributions is large. Therefore, separation of e, μ and π by their momenta is impossible at $\sqrt{s} > 600$ MeV.

On the contrary, the energy deposition of the particles in the calorimeter [17] is quite different for e, μ and π. The typical energy deposition of two particles (E^+ vs. E^-) for experimental events selected

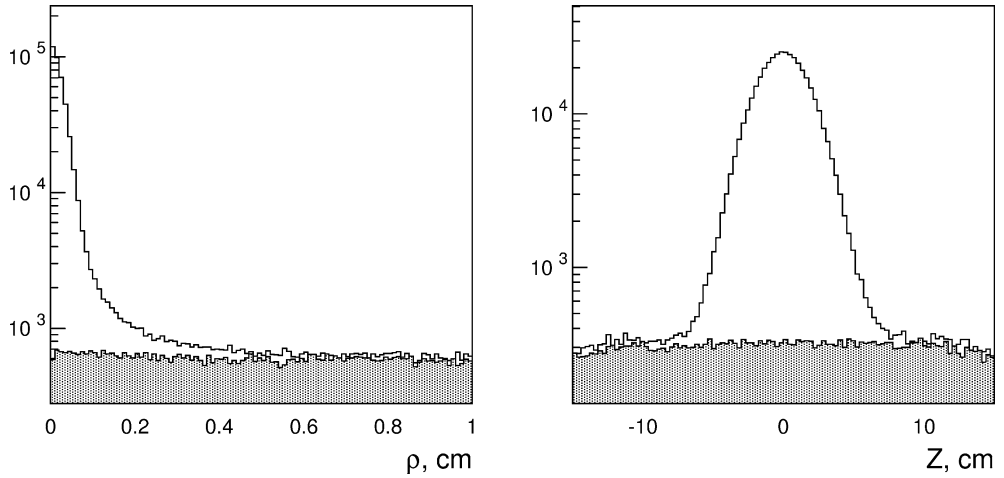

Fig. 1. Spatial distribution of the vertex. The left plot shows the distribution of the distance from the vertex to the beam axis (ρ), the right plot presents the distribution of the distance between the vertex and the center of the detector along the beam axis (z). The open histogram corresponds to all collinear events, the filled one shows the subset of background events.

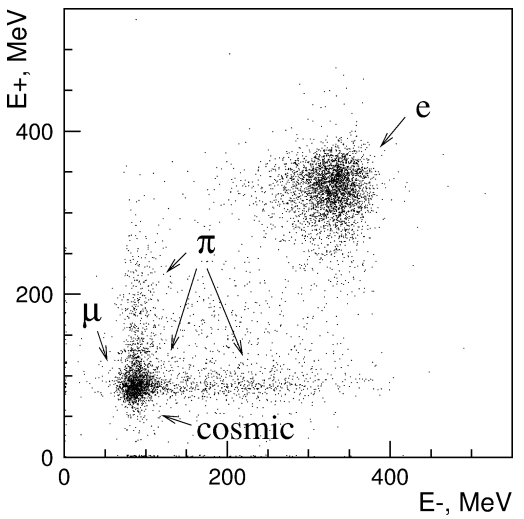

Fig. 2. Energy deposition of collinear events for the beam energy of 400 MeV.

at the beam energy of 400 MeV is shown in Fig. 2. The high deposition spot corresponds to e^+e^- pairs, where both particles leave almost all their energy in the calorimeter. The low deposition spot represents $\mu^+\mu^-$ pairs, cosmic muons and those $\pi^+\pi^-$ pairs, in which both particles interact as minimum-ionizing. The long tails correspond to $\pi^+\pi^-$ pairs in which one or both particles undergo nuclear interactions inside the calorimeter.

Therefore, the energy deposition of the particles was used for the separation of the beam originating events. Since the overlap of the distributions for e^+e^- and $\pi^+\pi^-$ pairs is small, this approach gives stable results with a small systematic error. However, $\mu^+\mu^-$ and $\pi^+\pi^-$ pairs cannot be separated well by their energy deposition. To avoid this problem, the number of $\mu^+\mu^-$ pairs was derived from the number of e^+e^- pairs according to QED, taking into account radiative corrections and detection efficiencies. Since in this energy range the number of $\mu^+\mu^-$ pairs is small compared to that of $\pi^+\pi^-$, the systematic error caused by the corresponding calculation is negligible (less than 0.03%).

The separation was based on the minimization of the following unbinned likelihood function:

$$L = -\sum_{\text{events}} \ln\left(\sum_a N_a \cdot f_a\left(E^+, E^-\right)\right) + \sum_a N_a, \tag{3}$$

where a is the event type ($a = ee$, $\mu\mu$, $\pi\pi$, cosmic), N_a is the number of events of the type a and $f_a(E^+, E^-)$ is the probability density function (p.d.f.) for a type a event to have energy depositions E^+ and E^-. It was assumed that E^+ and E^- are not correlated for events of the same type, so the p.d.f. can be factorized as

$$f_a\left(E^+, E^-\right) = f_a^+\left(E^+\right) \cdot f_a^-\left(E^-\right),$$

where $f_a^{\pm}(E)$ is the p.d.f. for $e^{\pm}$, $\mu^{\pm}$, $\pi^{\pm}$ and cosmic muons to have energy deposition equal to E. This assumption is not entirely correct since there are small correlations between E^+ and E^- because of the dependence of the calorimeter thickness on the polar angle as well as the c.m. energy shift due to the initial state radiation. The first effect was corrected for while the second one was studied with the help of simulation and was shown to be negligible (below 0.1%).

For e^+e^-, $\mu^+\mu^-$ pairs and cosmic events the energy deposition does not depend on the particle charge, while the energy depositions for π^+ and π^- are different. Therefore $f_a^+ \equiv f_a^-$ for $a = ee, \mu\mu$ and cosmic, but in case of pions the corresponding p.d.f.'s are different.

As was mentioned before, the ratio $N_{\mu\mu}/N_{ee}$ was fixed during minimization according to the QED calculation

$$\frac{N_{\mu\mu}}{N_{ee}} = \frac{\sigma_{\mu\mu}\cdot(1+\delta_{\mu\mu})\varepsilon_{\mu\mu}}{\sigma_{ee}\cdot(1+\delta_{ee})\varepsilon_{ee}},$$

where σ is the Born cross-section, δ is the radiative correction and ε is the detection efficiency which includes acceptance as well as reconstruction and trigger efficiencies. The number of cosmic events N_{cosmic} determined separately was fixed during the minimization while its fluctuation was added in quadrature to the fluctuation of $N_{\pi\pi}$.

To obtain the specific form of p.d.f.'s, the energy deposition of e, μ and π in the CMD-2 calorimeter was studied. For electrons (positrons) and cosmic muons it can be obtained with the help of the data itself. Particles of positive charge with large enough energy deposition are almost 100% positrons and they were used to tag electrons. Events with a large value of ρ are mostly cosmic muons. Such tagged particles were used to determine the energy deposition of electrons and cosmic muons, respectively.

The simulation was used to obtain the energy deposition of muons from $e^+e^- \to \mu^+\mu^-$. In the energy range under study these muons interact purely as minimum-ionizing particles which are well described by the simulation.

On the contrary, the simulation of the interaction of low energy pions inside the calorimeter is not reliable enough. In addition, there is no good method to tag pions from $e^+e^- \to \pi^+\pi^-$ events. Therefore, the p.d.f.'s for π^+ and π^- were obtained from the analysis of the energy deposition of pions coming from the $\phi(1020) \to \pi^+\pi^-\pi^0$ decay. From a large data sample collected by CMD-2 around the ϕ-meson peak, about 10^5 $\phi(1020) \to 3\pi$ events were selected with practically no background. Pions found in these events cover the whole interesting range of momenta and angles. The energy deposition of these pions was analyzed and the parameterization for π^+ and π^- p.d.f.'s was derived.

Finally, to simplify the final error calculation, the likelihood function (3) was rewritten to have the following global fit parameters:

$$(N_{ee} + N_{\mu\mu}), \qquad \frac{N_{\pi\pi}}{N_{ee} + N_{\mu\mu}},$$

instead of N_{ee} and $N_{\pi\pi}$ (with $N_{\mu\mu}/N_{ee}$ and N_{cosmic} fixed). The likelihood function has some other fit parameters characterizing the p.d.f.'s for different types of particles, such as the mean energy, energy resolution, the asymmetry of some distributions etc. More detail about the energy deposition of different types of collinear events and the p.d.f. parameterization can be found in [16].

After the separation procedure the following number of events was obtained for three described above classes: $N_{ee} + N_{\mu\mu} = 180038$, $N_{\pi\pi} = 113824$ and $N_{\text{cosmic}} = 17390$.

Special studies were performed to estimate the systematic error of the separation procedure. The dominant effect was produced by the small non-uniformity of the calorimeter calibration. Due to the forward–backward asymmetry of the $e^+e^- \to e^+e^-$ cross-section, the calorimeter calibration error leads to a small difference between e^+ and e^- energy depositions. The corresponding error was found to be less than 0.2%. Several different functional forms were used to parameterize p.d.f.'s of e's and π's and the final cross section was stable within 0.1% for different selections. The existing variation of the calorimeter response between calibrations leads to small variations of the energy resolution which could also influence the results. The estimated contribution of this effect is below 0.1%. As a final test, the large amount of $e^+e^- \to e^+e^-(\gamma)$, $\mu^+\mu^-(\gamma)$, $\pi^+\pi^-(\gamma)$ events was generated in a proper proportion with the help of full detector simulation at several energy points covering the whole energy range. After that the simulated events were subject to the same separation

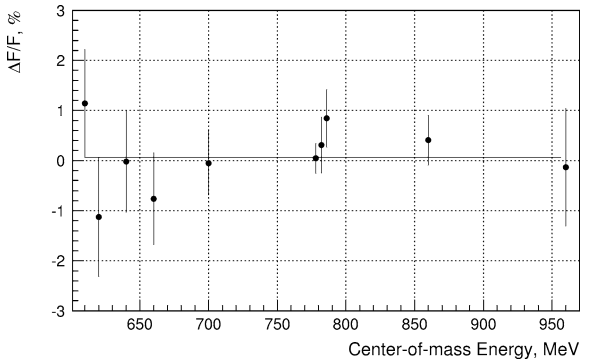

Fig. 3. Difference between the initial and the reconstructed values of the form factor for the simulated data set.

procedure as for the data. Results are shown in Fig. 3. The reconstructed value is always consistent with the input one and the average difference is below 0.1% or consistent with zero. Thus, the systematic error because of the event separation taking into account the above effects is estimated to be 0.2%.

3. Form factor calculation

The pion form factor was calculated as:

$$|F_\pi|^2 = \frac{N_{\pi\pi}}{N_{ee}+N_{\mu\mu}} \times \frac{\sigma_{ee}\cdot(1+\delta_{ee})\varepsilon_{ee}+\sigma_{\mu\mu}\cdot(1+\delta_{\mu\mu})\varepsilon_{\mu\mu}}{\sigma_{\pi\pi}\cdot(1+\delta_{\pi\pi})(1+\Delta_N)(1+\Delta_D)\varepsilon_{\pi\pi}} - \Delta_{3\pi}, \quad (4)$$

where the ratio $N_{\pi\pi}/(N_{ee}+N_{\mu\mu})$ was obtained from the minimization of (3), σ are the corresponding Born cross-sections, δ are the radiative corrections, ε are the detection efficiencies, Δ_D and Δ_N are the corrections for the pion losses caused by decays in flight and nuclear interactions, respectively, and $\Delta_{3\pi}$ is the correction for misidentification of $\omega\to\pi^+\pi^-\pi^0$ events as the $e^+e^-\to\pi^+\pi^-$. In the case of the $e^+e^-\to\pi^+\pi^-$ process, $\sigma_{\pi\pi}$ corresponds to point-like pions.

Radiative corrections were calculated according to Refs. [18,19] in which the accuracy of the obtained formulae was 0.2%.[2] The improved precision of the calculations compared to previous works [20] comes from taking into account the radiation of the additional photon in a narrow cone along the direction of electrons and positrons. The radiative corrections were calculated by the Monte Carlo integration of the differential cross-sections imposing all selection criteria. Analysis was repeated for three various sets of selection criteria corresponding to notably different radiative corrections. The obtained form factor values were consistent with each other. We estimate the uncertainty of the form factor because of the radiative corrections to be 0.4% dominated by the accuracy of the ratio $(1+\delta_{ee})/(1+\delta_{\pi\pi})$.

The radiative corrections for the process $e^+e^-\to\pi^+\pi^-$ include the effects of both initial (ISR) and final state radiation (FSR) and do not include the vacuum polarization terms (both leptonic and hadronic) since the latter are considered to be an intrinsic part of the hadronic cross-section and corresponding form factor (1). However, for various applications based on dispersion relations and involving the total cross-section of $e^+e^-\to$ hadrons, the radiation by final pions is no longer a radiative correction, so that $\pi^+\pi^-\gamma$ with a photon radiated by one of the final pions should be considered as one of the possible hadronic final states contributing to the total cross-section. Therefore, the bare cross-section $e^+e^-\to\pi^+\pi^-(\gamma)$, below referred to as $\sigma^0_{\pi\pi(\gamma)}$, was also calculated as

$$\sigma^0_{\pi\pi(\gamma)} = \frac{\pi\alpha^2}{3s}\beta_\pi^3\left|F_\pi(s)\right|^2\cdot\left|1-\Pi(s)\right|^2 \times\left(1+\frac{\alpha}{\pi}A(s)\right). \quad (5)$$

The factor $|1-\Pi(s)|^2$ with a polarization operator $\Pi(s)$ excludes the effect of leptonic and hadronic vacuum polarization, so that one obtains the bare cross-section required for various applications.[3] A correction for the final state radiation $A(s)$ was calculated based on [19], where only the effects of FSR, integrated over the whole allowed kinematic region, were

[2] We corrected a misprint in formula (2.5) of Ref. [19], also noted by the authors of Ref. [21].

[3] Note that the definition of the cross-section above is different from that in [16] where the FSR cross-section was not taken into account and only the correction for the leptonic vacuum polarization was applied. Therefore, their comparison is meaningless.

taken into account. The result

$$\Lambda(s) = \frac{1+\beta_\pi^2}{\beta_\pi}\left\{4\,\mathrm{Li}_2\left(\frac{1-\beta_\pi}{1+\beta_\pi}\right) + 2\,\mathrm{Li}_2\left(-\frac{1-\beta_\pi}{1+\beta_\pi}\right) - \left[3\ln\left(\frac{2}{1+\beta_\pi}\right) + 2\ln\beta_\pi\right]L_{\beta\pi}\right\} - 3\ln\left(\frac{4}{1-\beta_\pi^2}\right) - 4\ln\beta_\pi + \frac{1}{\beta_\pi^3}\left[\frac{5}{4}\left(1+\beta_\pi^2\right)^2 - 2\right]L_{\beta_\pi} + \frac{3}{2}\frac{1+\beta_\pi^2}{\beta_\pi^2}, \tag{6}$$

where $L_{\beta_\pi} = \ln\frac{1+\beta_\pi}{1-\beta_\pi}$, $\mathrm{Li}_2(z) = -\int_0^z \frac{dx}{x}\ln(1-x)$, coincides with [21,22].

Two different trigger settings were used during data taking. For energies below 810 MeV only a charged trigger was used in which the positive decision was based on the information from the tracking system only. The efficiency of the charged trigger was measured to be higher than 99% and, more important, equal for different types of collinear events in the energy range under consideration. Therefore, the uncertainties related to the trigger efficiency cancel in (4). Above 810 MeV the additional requirement that the energy deposition in the calorimeter be at least 20 MeV was applied for the trigger. The efficiency of this requirement was measured to be 99.5% for $e^+e^- \to \pi^+\pi^-$, 99.2% for $e^+e^- \to \mu^+\mu^-$ and 100% for $e^+e^- \to e^+e^-$ events, and was included in the corresponding detection efficiency. These corrections give a negligible contribution to the systematic uncertainty.

The reconstruction efficiency was measured using the experimental data themselves. It was found to be within the 98–100% range at all energies and, within the statistical accuracy, nearly the same for all types of collinear events. Therefore, it cancels in (4). The systematic error of the cancellation was estimated to be better than 0.2%. It is worth noting that such a cancellation allows a determination of the form factor with better precision than that of the luminosity.

The fiducial volume (detection solid angle) is determined by selecting events with the average polar angle $\Theta_{\mathrm{avr}} = (\Theta_1 + \pi - \Theta_2)/2$ in the range between $\Theta_{\min}$ and $(\pi - \Theta_{\min})$ with $\Theta_{\min} = 1.1$. The value of Θ_{avr} is determined by the CMD-2 Z-chamber [23] which has a spatial resolution along the beam axis better than 0.6 mm. That corresponds to a systematic error in the form factor of about 0.2%. To test this estimate, the pion form factor was also determined at $\Theta_{\min} = 1.0$ radian. The difference between the form factor values determined at two values of $\Theta_{\min}$ averaged over the c.m. energy range was found to be $(0.1 \pm 0.3)\%$, consistent with zero.

The correction Δ_D for the pion losses caused by decays in flight was calculated with the help of simulation. Its value, varying from 0.2% at 600 MeV to 0.03% around the $\phi(1020)$-meson, turned out to be small because of the small size of the decay volume and the fact that the maximum decay angle is small enough and of the same magnitude as the angular resolution of the drift chamber. This effect gives a negligible contribution to the systematic uncertainty.

The correction Δ_N for the pion losses caused by nuclear interactions inside the wall of the beam pipe or the drift chamber was calculated with the help of FLUKA-based simulation [24]. The value of the correction is slowly changing from 1.7% at 600 MeV to 0.8% at the $\phi(1020)$-meson energy. The systematic error of 0.2% for the Δ_N calculation was estimated from the uncertainty of the nuclear cross-sections used in FLUKA [25].

There is also a small correction for the losses of $e^+e^- \to e^+e^-$ events, caused by interactions of electrons with material of the beam pipe and the drift chamber. It was taken into account by reducing Δ_N by 0.15% according to the simulation.

Use of the resonance depolarization for the absolute beam energy calibration reduced the systematic uncertainty of the form factor due to the beam energy measurement to 0.1%.

In the narrow energy range around the $\omega(782)$-meson there is a small background of $e^+e^- \to \pi^+\pi^-\pi^0$ events, misidentified as $e^+e^- \to \pi^+\pi^-$. The corresponding correction $\Delta_{3\pi}$ was calculated from the simulation. It reaches its maximum value of about 1% at the $\omega(782)$-meson energy and drops fast to nearly zero at the energies outside the ω-meson.

The measured values of the pion form factor as well as those of the bare $e^+e^- \to \pi^+\pi^-(\gamma)$ cross-section obtained from (5) are shown in Table 1. Only statistical errors are given. The main sources of the systematic error are listed in Table 2. The overall system-

Table 1
The measured values of the pion form factor and bare cross-section $e^+e^- \to \pi^+\pi^-(\gamma)$. Only statistical errors are shown. The systematic error is estimated to be 0.6%

$2E$ (MeV)	$\lvert F_\pi\rvert^2$	$\sigma^0_{\pi\pi(\gamma)}$, nb
610.50	8.00 ± 1.13	327.8 ± 46.2
620.50	9.71 ± 0.72	390.6 ± 29.1
630.50	10.82 ± 0.73	426.9 ± 28.6
640.51	11.02 ± 0.72	426.2 ± 27.9
650.49	12.66 ± 0.83	480.3 ± 31.6
660.50	13.40 ± 0.75	498.8 ± 27.8
670.50	15.36 ± 0.82	560.5 ± 30.0
680.59	19.49 ± 0.90	697.2 ± 32.3
690.43	20.49 ± 0.73	718.6 ± 25.5
700.52	23.81 ± 0.62	818.1 ± 21.2
710.47	27.52 ± 0.99	926.1 ± 33.4
720.25	31.80 ± 0.82	1048.1 ± 27.0
730.24	34.34 ± 1.18	1107.2 ± 38.1
740.20	37.82 ± 1.18	1191.9 ± 37.1
750.28	42.33 ± 1.18	1302.9 ± 36.2
760.18	43.44 ± 1.21	1306.9 ± 36.5
764.17	43.23 ± 1.03	1289.6 ± 30.6
770.11	44.23 ± 1.14	1304.6 ± 33.5
774.38	43.19 ± 1.15	1265.7 ± 33.7
778.17	45.41 ± 1.29	1321.6 ± 37.7
780.17	42.90 ± 1.21	1234.9 ± 34.8
782.23	36.59 ± 0.66	1026.6 ± 18.5
784.24	34.30 ± 0.97	935.9 ± 26.5
786.04	30.01 ± 1.07	809.5 ± 28.9
790.10	31.96 ± 1.11	859.3 ± 30.0
794.14	29.81 ± 0.85	799.6 ± 22.7
800.02	29.40 ± 0.68	782.7 ± 18.1
810.14	25.60 ± 0.55	669.7 ± 14.4
820.02	24.09 ± 0.78	619.0 ± 20.0
829.97	20.52 ± 0.73	517.5 ± 18.5
839.10	16.75 ± 0.70	415.4 ± 17.3
849.24	14.16 ± 0.70	344.8 ± 17.0
859.60	14.47 ± 0.67	345.7 ± 15.9
869.50	11.10 ± 0.46	260.7 ± 10.7
879.84	10.13 ± 0.79	233.6 ± 18.1
889.72	8.44 ± 0.34	191.1 ± 7.7
900.04	7.74 ± 0.29	172.1 ± 6.4
910.02	6.82 ± 0.31	149.1 ± 6.8
919.56	6.03 ± 0.30	129.7 ± 6.5
930.11	5.70 ± 0.36	120.3 ± 7.7
942.19	5.16 ± 0.25	106.8 ± 5.1
951.84	4.56 ± 0.23	92.9 ± 4.8
961.52	4.29 ± 0.23	86.2 ± 4.6

atic error obtained by summing individual contributions in quadrature is about 0.6%. The values of the pion form factor and the bare cross-section in Table 1 supersede our preliminary results presented in Table 3 of Ref. [16].

Table 2
Main sources of the systematic errors

Source	Contribution (%)
Event separation	0.2
Radiative corrections	0.4
Detection efficiency	0.2
Fiducial volume	0.2
Correction for pion losses	0.2
Beam energy determination	0.1
Total	0.6

4. Fit to data

The parameterization of the pion form factor in the energy range under study should include contributions from the $\rho(770)$, $\omega(782)$ and $\rho(1450)$ resonances. It was assumed that the only mechanism for the $\omega \to \pi^+\pi^-$ decay is ρ–ω mixing. Following [26], we represent the wave function of the $\omega(782)$-meson as

$$|\omega\rangle = |\omega_0\rangle + \varepsilon|\rho_0\rangle\,,$$

where $|\omega_0\rangle$ and $|\rho_0\rangle$ are the pure isoscalar and isovector, respectively, and ε is the ρ–ω mixing parameter. Then, in the energy region close to the $\rho(770)$- and $\omega(782)$-meson masses, the form factor can be written as

$$F_\pi(s) = \left[\frac{F_\rho}{s - M_\rho^2} + \varepsilon\frac{F_\omega}{s - M_\omega^2}\right]\left[\frac{F_\rho}{-M_\rho^2} + \varepsilon\frac{F_\omega}{-M_\omega^2}\right]^{-1} \approx -\frac{M_\rho^2}{s - M_\rho^2}\left[1 + \varepsilon\frac{F_\omega(M_\omega^2 - M_\rho^2)s}{F_\rho M_\omega^2(s - M_\omega^2)}\right], \qquad (7)$$

where we keep only the terms linear in ε. The quantities M_ω and M_ρ are complex and contain the corresponding widths.

Combining together the contributions from the $\rho(770)$- and $\rho(1450)$-mesons, and including that from the $\omega(782)$-meson as in (7), we write the pion form factor:

$$F_\pi(s) = \left(\mathrm{BW}^{\mathrm{GS}}_{\rho(770)}(s)\cdot\left(1 + \delta\frac{s}{M_\omega^2}\mathrm{BW}_\omega(s)\right) + \beta\cdot\mathrm{BW}^{\mathrm{GS}}_{\rho(1450)}(s)\right)(1+\beta)^{-1}, \qquad (8)$$

where parameters δ and β describe the contributions of the $\omega(782)$- and $\rho(1450)$-mesons relative to the dominant one of the $\rho(770)$-meson. For the $\rho(770)$

and $\rho(1450)$ the GS parameterization is used [27]:

$$\mathrm{BW}^{\mathrm{GS}}_{\rho(M_\rho)} = \frac{M_\rho^2\left(1+d\cdot\Gamma_\rho/M_\rho\right)}{M_\rho^2 - s + f(s) - iM_\rho\Gamma_\rho(s)}, \tag{9}$$

where

$$f(s) = \Gamma_\rho\frac{M_\rho^2}{p_\pi^3(M_\rho^2)} \times\left[p_\pi^2(s)\big(h(s)-h\big(M_\rho^2\big)\big) + \big(M_\rho^2-s\big)p_\pi^2\big(M_\rho^2\big)\left.\frac{dh}{ds}\right|_{s=M_\rho^2}\right], \tag{10}$$

$$h(s) = \frac{2}{\pi}\frac{p_\pi(s)}{\sqrt{s}}\ln\frac{\sqrt{s}+2p_\pi(s)}{2m_\pi}, \tag{11}$$

and d is chosen to satisfy $\mathrm{BW}^{\mathrm{GS}}_{\rho(M_\rho)}(0)=1$:

$$d = \frac{3}{\pi}\frac{m_\pi^2}{p_\pi^2(M_\rho^2)}\ln\frac{M_\rho+2p_\pi(M_\rho^2)}{2m_\pi} + \frac{M_\rho}{2\pi p_\pi(M_\rho^2)} - \frac{m_\pi^2 M_\rho}{\pi p_\pi^3(M_\rho^2)}, \tag{12}$$

where M_ρ, Γ_ρ are the $\rho(770)$-meson mass and width, and $p_\pi(s)$ is the pion momentum at the squared c.m. energy s. For the energy dependence of the $\rho(770)$ width, the P-wave phase space is taken:

$$\Gamma_\rho(s) = \Gamma_\rho\left[\frac{p_\pi(s)}{p_\pi(M_\rho^2)}\right]^3\left[\frac{M_\rho^2}{s}\right]^{1/2}. \tag{13}$$

For the $\omega(782)$-meson contribution the simple Breit–Wigner parameterization with a constant width is used.

To obtain the $\rho(770)$-meson leptonic width $\Gamma(\rho\to e^+e^-)$, the well-known VDM relations were used [28]:

$$\Gamma_{V\to e^+e^-} = \frac{4\pi\alpha^2}{3M_V^3}g_{V\gamma}^2 \qquad \text{and}$$

$$\Gamma_{V\to\pi^+\pi^-} = \frac{g_{V\pi\pi}^2}{6\pi}\frac{p_\pi^3\big(M_V^2\big)}{M_V^2}. \tag{14}$$

Assuming

$$g_{\rho\gamma}g_{\rho\pi\pi} = \frac{M_\rho^2\big(1+d\cdot\Gamma_\rho/M_\rho\big)}{(1+\beta)} \qquad \text{and}$$

$$\Gamma_{\rho\to\pi^+\pi^-} = \Gamma_\rho, \tag{15}$$

the following result was obtained:

$$\Gamma_{\rho\to e^+e^-} = \frac{2\alpha^2 p_\pi^3(M_\rho^2)}{9M_\rho\Gamma_\rho}\frac{(1+d\cdot\Gamma_\rho/M_\rho)^2}{(1+\beta)^2}. \tag{16}$$

Similarly, assuming (14) and

$$g_{\omega\gamma}g_{\omega\pi\pi} = \frac{\delta\cdot M_\omega^2\cdot|\mathrm{BW}^{\mathrm{GS}}_{\rho(770)}(M_\omega^2)|}{(1+\beta)}, \tag{17}$$

the following expression is obtained for the branching ratio of the $\omega\to\pi^+\pi^-$ decay:

$$\mathrm{Br}\big(\omega\to\pi^+\pi^-\big) = \frac{2\alpha^2 p_\pi^3(M_\omega^2)}{9M_\omega\Gamma_{\omega\to e^+e^-}\Gamma_\omega}\big|\mathrm{BW}^{\mathrm{GS}}_{\rho(770)}\big(M_\omega^2\big)\big|^2\frac{|\delta|^2}{(1+\beta)^2}. \tag{18}$$

It should be mentioned that our parameterization of the $\omega(782)$-meson contribution is slightly different from that in [6,13]: $(1+\delta\cdot s/M_\omega^2\cdot\mathrm{BW}_\omega(s))$ instead of $(1+\delta\cdot\mathrm{BW}_\omega(s))/(1+\delta)$. Fits to either parameterization give the same result.

To estimate the model dependence of the obtained parameters, another model of the form factor parameterization was considered—the hidden local symmetry (HLS) model [28,29]. In this model the $\rho(770)$-meson appears as a dynamical gauge boson of a hidden local symmetry in the non-linear chiral Lagrangian. The $\rho(1450)$ contribution is not taken into account, replaced by the non-resonant coupling $\gamma\pi^+\pi^-$. This model introduces a real parameter a related to this non-resonant coupling. The original parameterization of the pion form factor was modified in a similar way to take into account the $\omega(782)$-meson contribution.

5. Results and discussion

5.1. $\rho(770)$- and $\omega(782)$-meson parameters

There are several parameters of both models whose values have to be taken from other measurements [30,31]. Their values were allowed to fluctuate within the stated experimental errors. The following values of the $\omega(782)$-meson parameters were taken from the CMD-2 experiment [31]: $M_\omega = (782.71\pm0.08)$ MeV, $\Gamma_\omega = (8.68\pm0.24)$ MeV, $\Gamma_{\omega ee} = (0.595\pm0.017)$ keV. Parameters of the $\rho(1450)$ were taken from [30]:

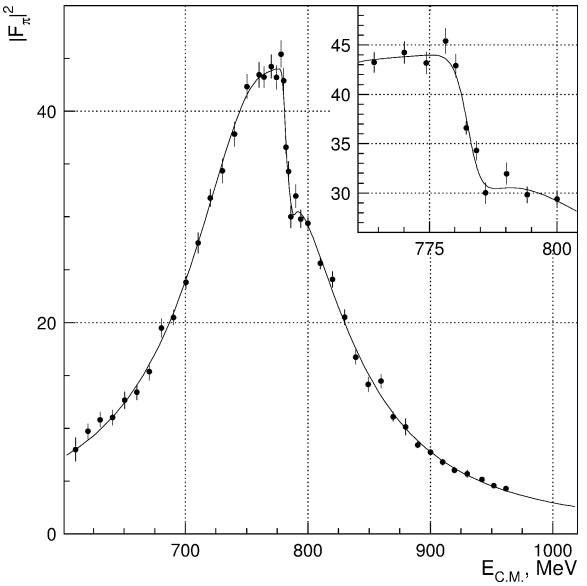

Fig. 4. Fit of the CMD-2 pion form factor data to the GS model.

$M_{\rho(1450)} = (1465 \pm 25)$ MeV and $\Gamma_{\rho(1450)} = (310 \pm 60)$ MeV.

Results of the fit in the GS model are shown in Fig. 4. Parameters of GS and HLS models obtained from the fit are in good agreement with each other and are shown in Table 3. The first error is statistical, the second one is systematic. Two effects were taken into account in the estimation of the latter: the systematic uncertainty of the form factor measurement of 0.6% (Table 2) and the contribution of the $\rho(1700)$ resonance missing in the adopted GS parameterization. The parameter β effectively describes the overall contribution of the $\rho(1450)$ and $\rho(1700)$ and its value is strongly correlated with the $\rho(1450)$ width. To extract the $\rho(1450)$ contribution, a fit of the data should be performed in a broader energy range. As a result, the value of β is strongly model dependent and is not well-defined in the energy range under study. For this reason, its systematic error is not shown.

In Table 4 the final results obtained in the GS model are compared to the world average values [30]. The values of the $\rho(770)$ mass and width shown there are based on the previous measurements at VEPP-2M [13], ALEPH [6] and CLEO [8]. While the mass of the $\rho(770)$ obtained in this Letter is in very good agreement with the previous measurements, our value of the width is 2.7 standard deviations lower. This difference can partly be explained by the difference of our parameterization compared to the previous works. Particularly, the value of Γ_ρ is correlated with the value of $\arg\delta$. In previous papers the parameter δ was assumed to be real. Fixing $\arg\delta = 0$ increases our value of Γ_ρ by 2 MeV. Such model uncertainties as the effect of the complex phase of δ and the difference between the results of GS and HLS fits were not included into the systematic error of the fit parameters.

The leptonic width of the $\rho(770)$ is in good agreement with the result of [13] quoted by [30]. Our value of the branching ratio $\omega \to \pi^+\pi^-$ is 1.6 standard deviations lower than the world average $(2.1 \pm 0.4)\%$ based on the two most precise measurements from e^+e^- experiments [13,32]. Again, a different parameterization of the form factor was used in previous works. Also note that the parameters of the $\omega(782)$-meson, such as mass, width and the leptonic width, have changed, that also affects the extracted value of the branching ratio. Our fit to the old data [13] gives

Table 3
Results from fits to $|F_\pi(s)|^2$ for the GS and HLS models

Parameter	GS model	HLS model
M_ρ (MeV)	$776.09 \pm 0.64 \pm 0.50$	$775.23 \pm 0.61 \pm 0.50$
Γ_ρ (MeV)	$144.46 \pm 1.33 \pm 0.80$	$143.88 \pm 1.44 \pm 0.80$
$\Gamma(\rho \to e^+e^-)$ (keV)	$6.86 \pm 0.11 \pm 0.05$	$6.84 \pm 0.12 \pm 0.05$
$\mathrm{Br}(\omega \to \pi^+\pi^-)$ (%)	$1.33 \pm 0.24 \pm 0.05$	$1.32 \pm 0.24 \pm 0.05$
$\lvert\delta\rvert$	$(1.57 \pm 0.15 \pm 0.05) \times 10^{-3}$	$(1.57 \pm 0.15 \pm 0.05) \times 10^{-3}$
$\arg\delta$	$12.6^\circ \pm 3.7^\circ \pm 0.2^\circ$	$13.0^\circ \pm 3.7^\circ \pm 0.2^\circ$
β (GS)	-0.0695 ± 0.0053	–
a (HLS)	–	$2.336 \pm 0.016 \pm 0.007$
χ^2/ν	0.92	0.94

Table 4
Comparison of the fit to $|F_\pi(s)|^2$ in the GS model to the world average values

Parameter	GS model	World average
M_ρ (MeV)	$776.09 \pm 0.64 \pm 0.50$	775.7 ± 0.7
Γ_ρ (MeV)	$144.46 \pm 1.33 \pm 0.80$	150.4 ± 1.6
$\Gamma(\rho \to e^+e^-)$ (keV)	$6.86 \pm 0.11 \pm 0.05$	6.77 ± 0.32
$\mathrm{Br}(\omega \to \pi^+\pi^-)$ (%)	$1.33 \pm 0.24 \pm 0.05$	2.1 ± 0.4

the value $\mathrm{Br}(\omega \to \pi^+\pi^-) = (2.00 \pm 0.34)\%$, still 1.6 standard deviations above our present result.

5.2. Hadronic contribution to the muon anomalous magnetic moment

Let us estimate the implication of our results for $a_\mu^{\pi\pi}$, the contribution from the annihilation into two pions, which dominates the hadronic contribution to $(g-2)/2$. To this end we compare its value in the energy range studied in this Letter and calculated from CMD-2 data only to that based on the previous e^+e^- measurements [13,32]. Table 5 presents results of the $a_\mu^{\pi\pi}$ calculations performed using formula (2) and the direct integration of the experimental data over the energy range studied in this Letter. As was explained above, the bare cross-section $\sigma^0_{\pi\pi(\gamma)}$ was used in the calculation. The method is straightforward and has been described elsewhere [3]. The first line of the Table 5 (Old data) gives the result based on the data of OLYA, CMD and DM1 while the second one (New data) is obtained from the CMD-2 data only. The third line (Old + new data) presents the weighted average of these two estimates. The assumption about the complete independence of the old and new data used in the averaging procedure seems to be well justified. For convenience, we list separately statistical and systematic uncertainties in the second column while the third one gives the total error obtained by adding them in quadrature. One can see that the estimate based on the CMD-2 data is in good agreement with that coming from the old data. It is worth noting that the statistical error of our measurement is slightly larger than the systematic uncertainty. Because of the small systematic error of the new data, the uncertainty of the new result for $a_\mu^{\pi\pi}$ is almost three times better than the previous one. As a result, the combined value based on both old and new data is completely dominated by the CMD-2 measurement.

Table 5
Contributions of the $\pi\pi$ channel to $(g-2)/2$

	$a_\mu^{\pi\pi}$, 10^{-10}	Total error, 10^{-10}
Old data	$374.8 \pm 4.1 \pm 8.5$	9.4
New data	$368.1 \pm 2.6 \pm 2.2$	3.4
Old + new data	$368.9 \pm 2.2 \pm 2.3$	3.2

The example above only illustrates the importance of the improved accuracy. At the present time the analysis of the $\pi\pi$ data as well as other hadronic final states in the whole energy range accessible to CMD-2 is in progress. Independent information is also available [33] or expected in close future from other experiments studying low energy e^+e^- annihilation [34]. When all the above mentioned data are taken into account, one can expect a significant improvement of the overall error of a_μ^{had} (by a factor of about 2) compared to the previous one based on the e^+e^- data only [3].

The completion of the analysis of the $\pi\pi$ data will also provide a possibility of the precise test of the CVC based relation between the cross-section of $e^+e^- \to \pi^+\pi^-$ and the spectral function in the decay $\tau^- \to \pi^-\pi^0\nu_\tau$. The solution of the problem of the possible deviation between e^+e^- and τ-lepton data [8,10] should also involve a thorough investigation of the effects of isospin breaking corrections as well as additional radiative corrections in τ decays [22,35,36].

6. Conclusion

The following values of the ρ- and ω-meson parameters have been obtained with the Gounaris–Sakurai fit to the formfactor data:

$$M_\rho = (776.09 \pm 0.64 \pm 0.50)\ \mathrm{MeV},$$

$$\Gamma_\rho = (144.46 \pm 1.33 \pm 0.80)\ \mathrm{MeV},$$

$$\Gamma\big(\rho \to e^+e^-\big) = (6.86 \pm 0.11 \pm 0.05)\ \mathrm{keV},$$

$$\mathrm{Br}\big(\omega \to \pi^+\pi^-\big) = (1.33 \pm 0.24 \pm 0.05)\%,$$

$$\arg\delta = 12.6^\circ \pm 3.7^\circ \pm 0.2^\circ.$$

The measurement presented in this Letter supersedes the preliminary result [16], obtained from the same

data. Analysis of the much larger data sample collected by CMD-2 in 1996 (the 370–540 MeV energy range), 1997 (the 1040–1380 MeV energy range) and 1998 (the second scan of the 370–960 MeV energy range) is in progress.

Acknowledgements

The authors are grateful to the staff of VEPP-2M for excellent performance of the collider, to all engineers and technicians who contributed to the CMD-2 experiment. We acknowledge numerous useful discussions with M. Benayoun, A. Höcker, F. Jegerlehner, W.J. Marciano, K.V. Melnikov and G.N. Shestakov.

This work is supported in part by grants DOE DEFG0291ER40646, INTAS 96-0624, Integration A0100, NSF PHY-9722600, NSF PHY-0100468 and RFBR-98-02-17851.

References

[1] T. Kinoshita, B. Nižić, Y. Okamoto, Phys. Rev. D 31 (1985) 2108.
[2] R.M. Carey et al., Phys. Rev. Lett. 82 (1999) 1632.
[3] S. Eidelman, F. Fegerlehner, Z. Phys. C 67 (1995) 585.
[4] M. Davier, A. Höcker, Phys. Lett. B 435 (1998) 427.
[5] Y.S. Tsai, Phys. Rev. D 4 (1971) 2821;
H.B. Thacker, J.J. Sakurai, Phys. Lett. B 36 (1971) 103.
[6] R. Barate et al., Z. Phys. C 76 (1997) 15.
[7] K. Ackerstaff et al., Eur. Phys. J. C 7 (1999) 571.
[8] S. Anderson et al., Phys. Rev. D 61 (2000) 112002.
[9] R. Alemany, M. Davier, A. Höcker, Eur. Phys. J. C 2 (1998) 123.
[10] S. Eidelman, Nucl. Phys. B (Proc. Suppl.) 98 (2001) 281.
[11] H.N. Brown et al., Phys. Rev. Lett. 86 (2001) 2227.
[12] M. Knecht, A. Nyffeler, hep-ph/0111058;
M. Hayakawa, T. Kinoshita, hep-ph/0112102;
I. Blokland, A. Czarnecki, K. Melnikov, hep-ph/0112117.
[13] L.M. Barkov et al., Nucl. Phys. B 256 (1985) 365.
[14] R.R. Akhmetshin et al., Preprint BudkerINP 99-11, Novosibirsk, 1999;
E.V. Anashkin et al., ICFA Instrumentation Bulletin 5 (1988) 18.
[15] A.P. Lysenko et al., Nucl. Instrum. Methods A 359 (1995) 419.
[16] R.R. Akhmetshin et al., Preprint INP 99-10, Novosibirsk, 1999, hep-ex/9904027.
[17] V.M. Aulchenko et al., Nucl. Instrum. Methods A 336 (1993) 53.
[18] A.B. Arbuzov et al., JHEP 10 (1997) 001.
[19] A.B. Arbuzov et al., JHEP 10 (1997) 006.
[20] F.A. Berends, R. Kleiss, Nucl. Phys. B 177 (1981) 237;
W. Beenakker, F.A. Berends, S.C. van der Marck, Nucl. Phys. B 349 (1991) 323.
[21] A. Hoefer, J. Gluza, F. Jegerlehner, Preprint DESY 00-163, 2001, hep-ph/0107154.
[22] K. Melnikov, Int. J. Mod. Phys. A 16 (2001) 4591.
[23] E.V. Anashkin et al., Nucl. Instrum. Methods A 323 (1992) 178.
[24] P.A. Aarnio et al., Technical report TIS-RP-190, CERN, 1987, 1990.
[25] A. Fasso et al., in: Proceedings of the Conference on Advanced Monte Carlo, Lisbon, 2000, p. 955;
A.M. Makhov, Preprint BudkerINP 92-66, Novosibirsk, 1992.
[26] R. Feynman, Photon–hadron Interactions, Benjamin, 1972, Chapter 6.
[27] G.J. Gounaris, J.J. Sakurai, Phys. Rev. Lett. 21 (1968) 244.
[28] M. Benayoun et al., Eur. Phys. J. C 2 (1998) 269.
[29] M. Bando et al., Phys. Rev. Lett. 54 (1985) 1215.
[30] D.E. Groom et al., Eur. Phys. J. C 15 (2000) 1, and 2001 off-year partial update, http://pdg.lbl.gov.
[31] R.R. Akhmetshin et al., Phys. Lett. B 476 (2000) 33.
[32] A. Quenzer et al., Phys. Lett. B 76 (1978) 512.
[33] J.Z. Bai et al., Phys. Rev. Lett. 84 (2000) 594;
J.Z. Bai et al., hep-ex/0102003.
[34] A. Aloisio et al., hep-ex/0107023;
E.P. Solodov, hep-ex/0107027.
[35] H. Czyż, J.H. Kühn, Eur. Phys. J. C 18 (2001) 497.
[36] V. Cirigliano, G. Ecker, H. Neufeld, Phys. Lett. B 513 (2001) 361.